Acta Crystallographica Section D
Biological Crystallography
ISSN 0907-4449

Unusual twinning in an acetyl coenzyme A synthetase (ADP-forming) from *Pyrococcus furiosus*

Lari Lehtiö,[a,b] Igor Fabrichniy,[a] Thomas Hansen,[c] Peter Schönheit[c] and Adrian Goldman[a]*

[a]Structural Biology and Biophysics, Institute of Biotechnology, University of Helsinki, Viikinkaari 1, PO Box 65, FIN-00014 University of Helsinki, Finland, [b]National Graduate School in Informational and Structural Biology, Finland, and [c]Institut für Allgemeine Mikrobiologie, Christian-Albrechts-Universität Kiel, Am Botanischen Garten 1-9, D-24118 Kiel, Germany

Correspondence e-mail: adrian.goldman@helsinki.fi

Received 26 October 2004
Accepted 28 December 2004

A recombinant form of an acetyl coenzyme A synthetase (ADP-forming) from *Pyrococcus furiosus* has been crystallized. Crystallization was accomplished by the sitting-drop vapour-diffusion technique. Crystals belong to the monoclinic space group *C*2, with unit-cell parameters $a = 131.3$, $b = 186.1$, $c = 121.5$ Å, $\beta = 122.6^\circ$, and diffract to 2.0 Å resolution on a synchrotron-radiation source. The unit-cell parameters allow twinning to the higher apparent space-group symmetry *F*222 by twin-lattice quasi-symmetry. The twinning fraction for the data is close to 40%. Two other data sets in the PDB show similar twinning.

1. Introduction

ADP-forming acetyl-CoA synthetase (ACD; EC 6.2.1.13) is a novel enzyme of acetate formation in archaea (Schäfer *et al.*, 1993) and a few eukaryotic protists, including the two eukaryotic human parasites *Entamoeba histolytica* (Reeves *et al.*, 1977; Field *et al.*, 2000) and *Giardia lamblia* (Sánchez *et al.*, 2000). *In vivo*, this unusual synthetase catalyses the conversion of acetyl-CoA to acetate and couples this reaction with the synthesis of ATP *via* substrate-level phosphorylation,

$$\text{acetyl-CoA} + \text{ADP} + \text{P}_\text{i} \rightarrow \text{acetate} + \text{ATP} + \text{CoA}.$$

The one-step conversion of acetyl-CoA to acetate coupled with ATP synthesis is unusual in prokaryotes and appears to be restricted to the archaea; all acetate-forming bacteria studied so far utilize phosphate acetyltransferase and acetate kinase for acetate formation and ATP synthesis (Bock *et al.*, 1999). ACD belongs to the NDP-forming acyl-CoA synthetase superfamily, which also includes succinyl CoA synthetases (Sánchez *et al.*, 2000).

In the hyperthermophilic archaea, the enzyme has been characterized from *Pyrobaculum aerophilum* (Bräsen & Schönheit, 2004) and *Methanococcus jannaschii* (Musfeldt & Schönheit, 2002) and two isoenzymes have been analyzed from *Pyrococcus furiosus* (Mai & Adams, 1996; Glasemacher *et al.*, 1997) and from *Archaeoglobus fulgidus* (Musfeldt & Schönheit, 2002). The isoenzymes of *P. furiosus*, ACD I and ACD II, function as acyl-CoA synthetases (ADP-forming) and differ in their specificities and kinetic constants toward acetyl-CoA/acetate and various acyl-CoA esters and their corresponding acids (Musfeldt & Schönheit, 2002). Both ACD isoforms are 145 kDa heterotetramers ($\alpha_2\beta_2$) composed of two subunits, α (47 kDa) and β (25 kDa).

Even though ACDs from various sources have been characterized, the structure of the enzyme has remained undetermined. Here, we report the crystallization of one of them: ACD I from *P. furiosus*. The structure should elucidate the functional and evolutionary differences between acetyl-CoA synthetases and provide a basis for further biochemical analysis of the enzymes and a deeper understanding of the reaction mechanism of this novel synthetase.

2. Materials and methods

2.1. Crystallization of ACD

The protein was purified as described previously (Musfeldt *et al.*, 1999) and initial crystals were obtained with a sparse-matrix screen (Jancarik & Kim, 1991) based on Hampton Research conditions. Crystallization conditions were further optimized by grid-screening

the precipitant concentrations and additives. Experiments were performed using the sitting-drop vapour-phase equilibration method at room temperature. 5 µl drops containing 30 mg ml^{-1} protein solution and precipitant solution in a ratio of 3:2 were placed in sitting-drop plates (Chryschem), sealed with tape and equilibrated against 0.5 ml well solution.

2.2. Data collection and analysis

Crystals were picked up from the drop with a nylon loop and flash-cooled in a nitrogen stream. X-ray data were collected at the ESRF ID14-EH3 beamline using a wavelength of 0.931 Å and a MAR CCD detector. Space-group assignment and data processing were performed with the *XDS* program package (Kabsch, 1993). Twinning was analysed with *DETWIN* and *TRUNCATE* from the *CCP*4 program package (Collaborative Computational Project, Number 4, 1994) and *DATAMAN* from the Uppsala Software Factory (Kleywegt & Jones, 1996).

3. Results and discussion

The best diffracting crystals were obtained from a sitting drop composed of 3 µl protein solution (30 mg ml^{-1}) and 2 µl well solution. The protein solution also contained 1 m*M* CoA and 2 m*M* AMPPcP (an ATP homologue). The well solution contained 0.1 *M* cacodylate pH 6.5, 35% MPD, 0.4 *M* sodium acetate and 5 m*M* $MgCl_2$. Crystals were obtained in a week and were approximately 50 × 50 × 100 µm in size (Fig. 1*a*). The crystallization condition contained a high concentration of MPD and the crystals could be flash-cooled directly after picking them up from the drop with a nylon loop. Crystals are typically red, although different conditions yielded colourless crystals that were not of diffraction quality. The reddish colour probably arises from loosely bound iron in the protein.

The crystals diffract quite weakly and we were unable to collect usable diffraction data using a rotating-anode X-ray source. At the synchrotron beamline we were generally able to obtain diffraction beyond 3 Å resolution. The best resolution so far, 2 Å, was obtained from a crystal grown in the presence of magnesium (Fig. 2). We have also collected derivative data from crystals grown in the presence of samarium (BM7A, Hamburg) and in the presence of mercury (BM7A, Hamburg and BM14, ESRF). The apparent space group of the crystals is orthorhombic *F*222, which results from twinning. The real space group of the crystals is *C*2. The unit-cell parameters of the *C*2 cell (a = 131.3, b = 186.1, c = 121.5 Å, β = 122.6°) follow the $\cos\beta = |na|/2|c|$ rule (Giacovazzo, 2002) and therefore twinning by the operator $hkl \rightarrow -h, -k, h + l$ is possible (Fig. 1*b*). Twinning is also

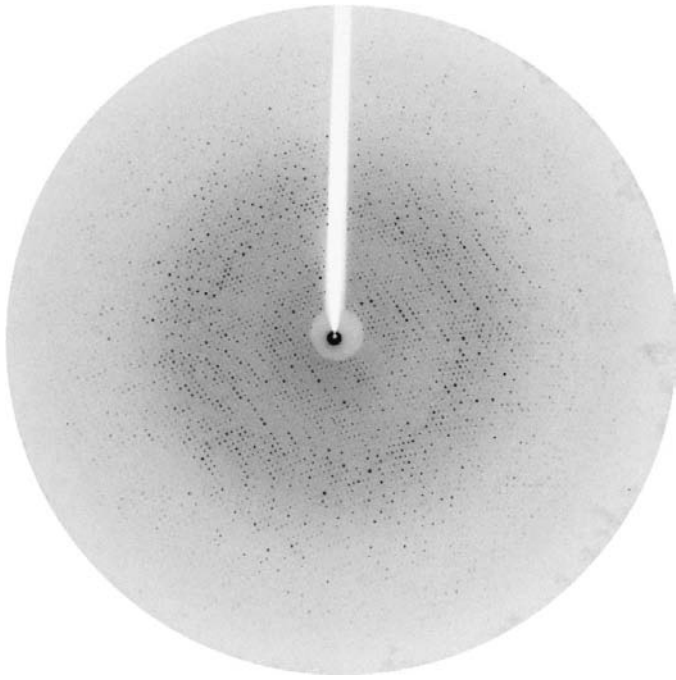

Figure 2
Oscillation image collected at ESRF beamline ID14-3. The oscillation range of an image is 0.5° and the edge of the image corresponds to a resolution of 1.78 Å.

evident from the cumulative intensity distribution statistics, which show a sigmoidal curve (Fig. 3*a*). In addition, the anomalous signal of a mercury derivative (data not shown) disappears when data are merged to *F*222, consistent with the twinning operator averaging non-Friedel mates together. The $R_{\rm merge}$ between different data sets generally is greater than 30% and is sometimes even above 60%, suggesting that the twinning fraction varies. However, for all the data sets we have collected so far the twinning fraction appears to be close to 40% (Fig. 3*b*). Estimation of the twin fraction from a crystal with high twin fraction is not very reliable owing to errors in the data (Goldman *et al.*, 1987).

Some of the twinning indicators gave contradictory results. The second moment of $\langle I\rangle$, the ratio of the average-squared intensities to square of the average intensities, should be 2 for untwinned acentric data and 1.5 for a perfect twin. For our data, the value is 2.3, which is too large for untwinned data. One explanation is pseudo-centring (Padilla & Yeates, 2003), but this is not indicated by the parity test. A recently introduced method of detecting twinning based on local intensity differences (Padilla & Yeates, 2003) indicates that the data are partially twinned (Fig. 3*c*). The values of $\langle|L|\rangle$ and $\langle L^2\rangle$ are 0.445 and 0.27, respectively. For untwinned data these should be 0.5 and 0.333 and for perfectly twinned data 0.375 and 0.200, respectively. The twinning fraction calculated only for the high-resolution data is always about 28% and the local intensity plot is also consistent with the high twinning fraction (data not shown).

The Matthews coefficient suggests that there are two to four $\alpha\beta$ heterodimers in the *C*2 asymmetric unit, corresponding to a Matthews coefficient of 4.1–2.1 Å Da^{-1} and a solvent content of 70–38%. The features in the self-rotation function are not pronounced, but the *F*222 symmetry is

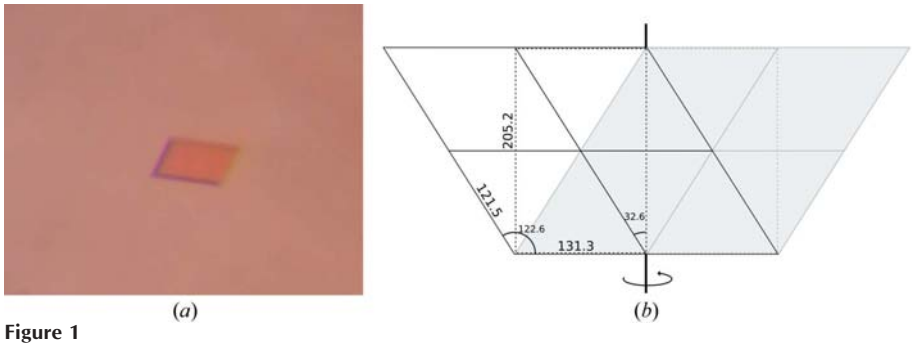

Figure 1
(*a*) A crystal of *P. furiosus* acetyl coenzyme A synthetase (ADP-forming) grown in a sitting drop. (*b*) Twinning from *C*2 to *F*222. The *xz* plane of the *C*2 lattice is shown in solid lines and the rectangular *F*222 lattice in dashed lines. The twin axis (marked) is along the long edge of the *F*222 cell. The two twin-related *C*2 lattices are shown in white and grey, respectively. Unit-cell parameters are shown in the figure in angstroms and degrees.

evident. All the Patterson maps have a peak at (0.03, 0, 0.06). In the native Patterson map, the peak is approximately half the height of the origin peak in all the data sets. Although a peak of this height may indicate translational symmetry between molecules in the asymmetric unit or a twofold axis running parallel to the crystallographic axis, the peak is too close to the origin for this to be the case. We therefore assume that it is an origin ripple or may arise from the twinning, as the twin axis passes through this point (Fig. 1*b*).

Rudolph *et al.* (2004) recently analysed a similar kind of monoclinic twinning in the primitive $P2_1$ lattice and found that of 2352 entries in the PDB, 77 had lattice parameters that would allow twinning mimicking orthorhombic symmetry with the twinning operator $hkl \rightarrow -h, -k, h + l$. There are no reports of $C2 \rightarrow F222$ twinning in macromolecular crystallography and so we analysed which of the $C2$ structures in the PDB have unit-cell parameters that would allow it. In contrast to the frequently encountered $C2$ space group (1704 entries), the apparent space group $F222$ is rather unusual, with only 23 entries. We used similar criteria to Rudolph *et al.* (2004) and included all the $C2$ entries with $2c|\cos\beta|/na$ or $2a|\cos\beta|/nc$ greater than 0.97 and smaller than 1.04. In all the entries that fulfilled these requirements n was 1. We found 25 unique protein structures (35 in total) from the PDB that could be twinned with an $hkl \rightarrow -h, -k, h + l$ operator and mimic $F222$ symmetry (Table 1).

Only one of the references related to the PDB entries described the possibility of scaling the data to $F222$ (Ursby *et al.*, 1999), but with a significantly higher merging R factor (9 and 40% with $C2$ and $F222$, respectively). In the case of ACD the twinning fraction is so high that it makes it possible to scale the data to $F222$ with reasonable statistics (Table 2). None of the articles related to the PDB entries describe twinned data. We tested twinning indicators for those entries that had structure factors available (Table 1). Only three of them had even a slightly sigmoidal cumulative intensity distribution and none of them had a second moment of I that was clearly below 2. For four entries, the second moment was greater than 2 as in our case. Finally, we analysed twinning with Britton plots using the twinning operator $hkl \rightarrow -h, -k, h + l$. Only two of the structures tested positive, with rather high overall twinning fractions of 34 and 40% for all data. In both cases the twinning fraction calculated with high-resolution data only is lower but not zero (10–14% for 1o0i and 28% for 1r0d), suggesting that at low resolution the structures are pseudo-$F222$, leading to a twinned $C2$ lattice at high resolution. Both of the structures are yet to be published.

The kind of pseudo-merohedral twinning described here is possible in monoclinic space groups and it makes them mimic the orthorhombic C-centred lattice in the case of $P2$ or $P2_1$ and the F-centred lattice in the case of $C2$. Rudolph *et al.* (2004) found only four $P2_1$ structures in the PDB twinned by the cosine rule. Similar twinning in $C2$ seems to be even rarer, since to the best of our knowledge there are no publications describing this kind of twinning in protein crystals. In order to overcome this rare case of twinning, we are screening for crystals to find a crystal with a low twin fraction that would enable us to solve the phase problem. We are also crystallizing homologous proteins, the structure of which might enable us to solve the structure

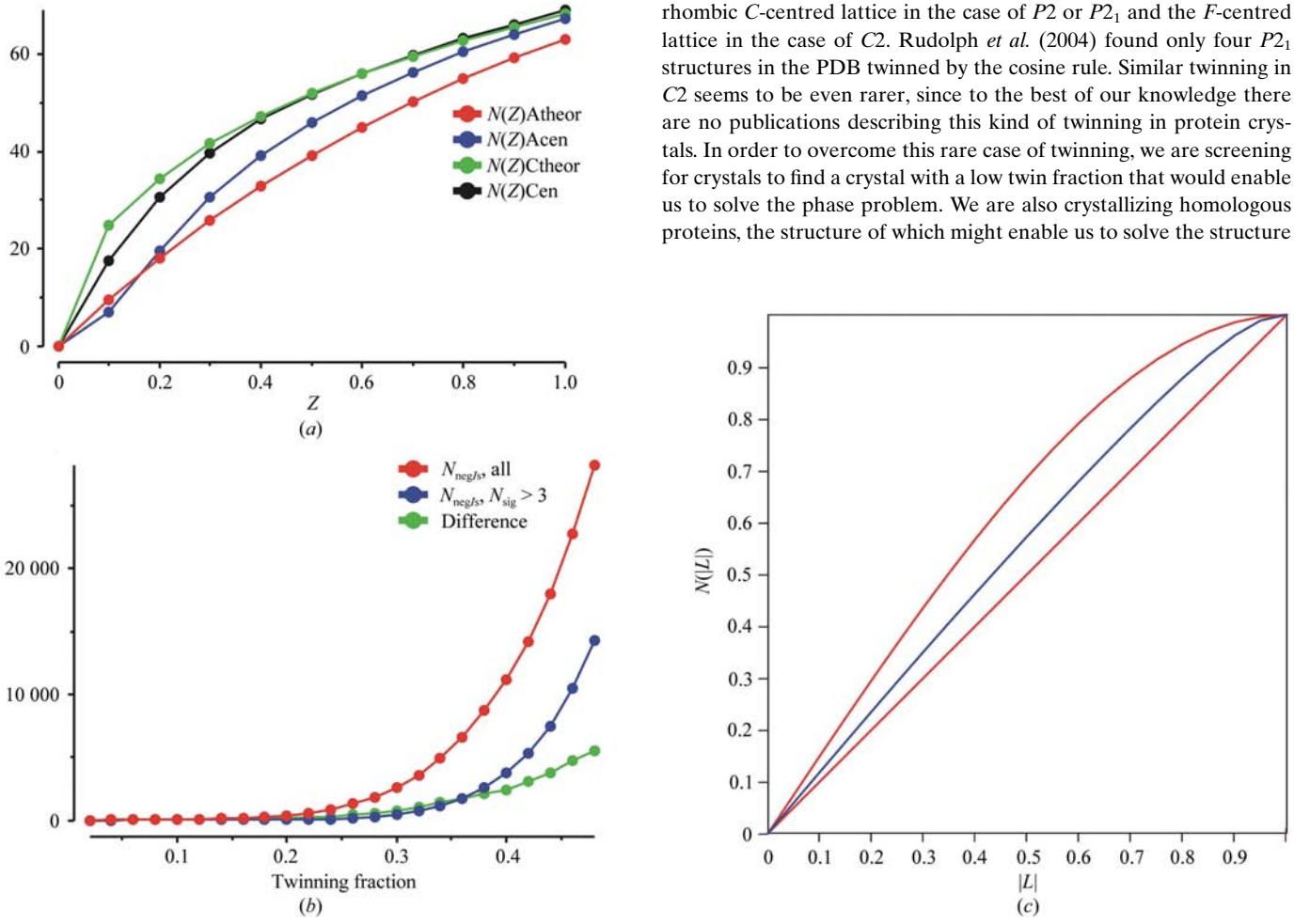

Figure 3
(*a*) Cumulative intensity distribution for the data processed to 2 Å shows that the amount of weak reflections is lower than expected from the theoretical value, resulting in a slightly sigmoidal curve. Theoretical distributions are in red and green and experimental distributions in blue and black for acentric and centric data, respectively. (*b*) A Britton plot (Fisher & Sweet, 1980) shows that the number of negative intensities starts to grow almost linearly only after the twinning fraction is close to 40%. The curve for all data is in red, that for the data for which $\langle N_{sig}\rangle I > 3$ in blue and their difference in green. (*c*) Local intensity difference statistics. $L = (I_1 - I_2)/(I_1 + I_2)$, where I_1 and I_2 are unrelated intensities and $N(|L|)$ is the cumulative probability distribution. The blue curve is the experimental data, the red line indicates the normal data and the red curve perfectly twinned data.

Table 1
Refinement statistics for unique PDB entries fulfilling the $2c|\cos\beta|/a = 1$ or $2a|\cos\beta|/c = 1$ rule.

SF +/− denotes whether or not structure factors were deposited to the PDB; CID +/− denotes whether or not the cumulative intensity distribution indicates twinning; Britton is the estimation of twin fraction with the operator $hkl \rightarrow -h, -k, h + l$.

PDB code	R (%)	R_{free} (%)	Resolution (Å)	SF	CID +/−	$\langle I^2\rangle/\langle\|I\|\rangle^2$	Britton (%)	Reference
1ank	20.1	31.6	2	−				Berry *et al.* (1994)
1b5t	21.2	26.3	2.5	−				Guenther *et al.* (1999)
1bl8	28	29	3.2	+	−	>2	−	Doyle *et al.* (1998)
1bu5	16.7	20.2	1.83	−				Walsh *et al.* (1998)
1et6	21.9	24.6	1.9	+	−	2	−	Arcus *et al.* (2000)
1hfo	22.5	28.1	1.65	+	+	2	−	Tan *et al.* (2001)
1hqd	15.4	20.3	2.3	+	−	2	−	Luic *et al.* (2001)
1i7z	22	26.5	2.3	+	−	2	−	Larsen *et al.* (2001)
1lfk	20.3	23.5	1.7	+	−	2	−	Zerbe *et al.* (2002)
1lw1	18.4	28.6	2.3	+	+	>2	−	Koshkin *et al.* (2003)
1np7	20.8	23.3	1.9	−				Brudler *et al.* (2003)
1nyt	13.6	16.9	1.5	+	−	2	−	Michel *et al.* (2003)
1o0i	18.5	22.8	1.7	+	−	−	34	Kuzin *et al.*, not published
1or7	19.9	23.1	2	+	−	2	−	Campbell *et al.* (2003)
1ots	26.4	29.9	2.5	+	−	2	−	Dutzler *et al.* (2003)
1p1j	16.5	19	1.7	+	−	2	−	Jin & Geiger (2003)
1q5x	22.6	27.4	2	−				Monzingo *et al.* (2003)
1r0d	22.4	26.9	1.9	+	−	>2	40	Brett *et al.*, not published
1sk7	23.5	27.3	1.6	−				Friedman *et al.* (2004)
1sss	16.6	19.6	2.3	+	−	2	−	Ursby *et al.* (1999)
1sx6	19.5	24.4	1.95	+	+	2	−	Malinina *et al.* (2004)
1ufk	23.2	25	1.9	+	−	>2	−	Kaminishi *et al.*, not published
1usg	19.1	21.6	1.53	+	−	2	−	Magnusson *et al.* (2004)
1vfh	19.7	25.2	2	−				Noda *et al.* (2004)
3pgk	−	−	2.5	−				Watson *et al.* (1982)

Table 2
Statistics for the data processed in *C*2 and in *F*222.

All data above an $I/\sigma(I)$ of −3 was included. Values for the highest resolution shell (2.1–2.0 Å) are in parentheses.

Space group	*C*2	*F*222
Unit-cell parameters		
a (°)	131.3	131.2
b (Å)	186.1	185.9
c (Å)	121.5	204.6
β (°)	122.6	
Diffraction range (Å)	20.0–2.0	20.0–2.0
No. observations	397212 (56731)	391027 (56514)
No. unique reflections	155026 (21996)	82143 (11311)
Redundancy	2.6 (2.6)	4.8 (5.0)
Completeness (%)	93.8 (98.1)	97.9 (100.0)
$I/\sigma(I)$	7.7 (3.1)	9.4 (4.1)
R_{merge}† (%)	9.8 (33.0)	11.9 (40.9)

† $R_{merge} = \sum_i |I_i - \langle I\rangle|/\sum\langle I\rangle$, where I is an individual intensity measurement and $\langle I\rangle$ is the average intensity for this reflection with summation over all data.

of this particular acetyl-CoA synthetase by molecular replacement using the twinned data.

Note added in proof. The recently reported crystal structure of a polymeric immunoglobulin binding fragment (Hamburger *et al.*, 2004) is another example of a structure solution where data exhibits *P*21 to *C*2221 twinning with a similar twinning operator to that discussed here.

This work was supported by grants from the Academy of Finland (172168, 178376 and 1105157 to AG and 1204363 to IF) and by the Sigrid Juselius foundation. LL is a member of the Informational and Structural Biology Graduate School. Beamtime was made available under the European Union Improving Human Potential Programme (Access to Research Infrastructures) at EMBL/DESY Hamburg under contract No. HPRI-CT-1999-00017 and at the ESRF under contract No. HPRI-CT-1999-00022. We thank Drs Andrea Schmidt and Gavin Fox for providing support at the EMBL/DESY and ESRF, respectively. We also thank Dr Veli-Matti Leppänen, Dr Tomi Airanne, MSc Veli-Pekka Jaakola and MSc Mika Rantanen for help collecting data and Esko Oksanen for discussions concerning evil twins. Finally, we thank the reviewers for their helpful comments.

References

Arcus, V. L., Proft, T., Sigrell, J. A., Baker, H. M., Fraser, J. D. & Baker, E. N. (2000). *J. Mol. Biol.* **299**, 157–168.
Berry, M. B., Meador, B., Bilderback, T., Liang, P., Glaser, M. & Phillips, G. N. Jr (1994). *Proteins*, **19**, 183–198.
Bock, A.-K., Glasemacher, J., Schmidt, R. & Schönheit, P. (1999). *J. Bacteriol.* **181**, 1861–1867.
Bräsen, C. & Schönheit, P. (2004). *Arch. Microbiol.* **182**, 277–287.
Brudler, R., Hitomi, K., Daiyasu, H., Toh, H., Kucho, K., Ishiura, M., Kanehisa, M., Roberts, V. A., Todo, T., Tainer, J. A. & Getzoff, E. D. (2003). *Mol. Cell*, **11**, 59–67.
Campbell, E. A., Tupy, J. L., Gruber, T. M., Wang, S., Sharp, M. M., Gross, C. A. & Darst, S. A. (2003). *Mol. Cell*, **11**, 1067–1078.
Collaborative Computational Project, Number 4 (1994). *Acta Cryst.* D**50**, 760–763.
Doyle, D. A., Morais Cabral, J., Pfuetzner, R. A., Kuo, A., Gulbis, J. M., Cohen, S. L., Chait, B. T. & MacKinnon, R. (1998). *Science*, **280**, 69–77.
Dutzler, R., Campbell, E. B. & Mackinnon, R. (2003). *Science*, **300**, 108–112.
Field, J., Rosenthal, B. & Samuelson, J. (2000). *Mol. Microbiol.* **38**, 446–455.
Fisher, R. G. & Sweet, R. M. (1980). *Acta Cryst.* A**36**, 755–760.
Friedman, J., Lad, L., Li, H., Wilks, A. & Poulos, T. L. (2004). *Biochemistry*, **43**, 5239–5245.
Giacovazzo, C. (2002). Editor. *Fundamentals of Crystallography*. Oxford University Press.
Glasemacher, J., Bock, A. K., Schmid, R. & Schönheit, P. (1997). *Eur. J. Biochem.* **244**, 561–567.
Goldman, A., Ollis, D. L. & Steitz, T. A. (1987). *J. Mol. Biol.* **194**, 143–153.
Guenther, B. D., Sheppard, C. A., Tran, P., Rozen, R., Matthews, R. G. & Ludwig, M. L. (1999). *Nature Struct. Biol.* **6**, 359–365.
Hamburger, A. E., West, A. P. Jr & Bjorkman, P. J. (2004). *Structure*, **12** 1925–1935.
Jancarik, J. & Kim, S.-H. (1991). *J. Appl. Cryst.* **24**, 409–411.
Jin, X. & Geiger, J. H. (2003). *Acta Cryst.* D**59**, 1154–1164.
Kabsch, W. (1993). *J. Appl. Cryst.* **26**, 795–800.
Kleywegt, G. J. & Jones, T. A. (1996). *Acta Cryst.* D**52**, 826–828.
Koshkin, A., Nunn, C. M., Djordjevic, S. & Ortiz De Montellano, P. R. (2003). *J. Biol. Chem.* **278**, 29502–29508.
Larsen, N. A., Zhou, B., Heine, A., Wirsching, P., Janda, K. D. & Wilson, I. A. (2001). *J. Mol. Biol.* **311**, 9–15.
Luic, M., Tomic, S., Lescic, I., Ljubovic, E., Sepac, D., Sunjic, V., Vitale, L., Saenger, W. & Kojic Prodic, B. (2001). *Eur. J. Biochem.* **268**, 3964–3973.
Magnusson, U., Salopek-Sondi, B., Luck, L. A. & Mowbray, S. L. (2004). *J. Biol. Chem.* **279**, 8747–8752.
Mai, X. & Adams, M. W. (1996). *J. Bacteriol.* **178**, 5897–5903.
Malinina, L., Malakhova, M. L., Teplov, A., Brown, R. E. & Patel, D. J. (2004). *Nature (London)*, **430**, 1048–1053.
Michel, G., Roszak, A. W., Sauve, V., Maclean, J., Matte, A., Coggins, J. R., Cygler, M. & Lapthorn, A. J. (2003). *J. Biol. Chem.* **278**, 19463–19472.
Monzingo, A. F., Gao, J., Qiu, J., Georgiou, G. & Robertus, J. D. (2003). *J. Mol. Biol.* **332**, 1015–1024.
Musfeldt, M. & Schönheit, P. (2002). *J. Bacteriol.* **184**, 636–644.
Musfeldt, M., Selig, M. & Schönheit, P. (1999). *J. Bacteriol.* **181**, 5885–5888.
Noda, M., Matoba, Y., Kumagai, T. & Sugiyama, M. (2004). *J. Biol. Chem.* **279**, 46153–46161.
Padilla, J. E. & Yeates, T. O. (2003). *Acta Cryst.* D**59**, 1124–1130.

Reeves, R. E., Warren, L. G., Süsskind, B. & Lo, H. S. (1977). *J. Biol. Chem.* **252**, 726–731.
Rudolph, M. G., Wingren, C., Crowley, M. P., Chien, Y. & Wilson, I. A. (2004). *Acta Cryst.* D**60**, 656–664.
Sánchez, L. B., Galperin, M. Y. & Müller, M. (2000). *J. Biol. Chem.* **275**, 5794–5803.
Schäfer, T., Selig, M. & Schönheit, P. (1993). *Arch. Microbiol.* **159**, 72–83.
Tan, T. H., Edgerton, S. A., Kumari, R., Mcalister, M. S., Rowe, S. M., Nagl, S., Pearl, L. H., Selkirk, M. E., Bianco, A. E., Totty, N. F., Engwerda, C., Gray, C. A. & Meyer, D. J. (2001). *Biochem. J.* **357**, 373–383.
Ursby, T., Adinolfi, B. S., Al-Karadaghi, S., De Vendittis, E. & Bocchini, V. (1999). *J. Mol. Biol.* **286**, 189–205.
Walsh, M. A., McCarthy, A., O'Farrell, P. A., McArdle, P., Cunningham, P. D., Mayhew, S. G. & Higgins, T. M. (1998). *Eur. J. Biochem.* **258**, 362–371.
Watson, H. C., Walker, N. P., Shaw, P. J., Bryant, T. N., Wendell, P. L., Fothergill, L. A., Perkins, R. E., Conroy, S. C., Dobson, M. J., Tuite, M. F., Kingsman, A. S. & Kingsman, S. M. (1982). *EMBO J.* **1**, 1635–1640.
Zerbe, K., Pylypenko, O., Vitali, F., Zhang, W., Rouset, S., Heck, M., Vrijbloed, J. W., Bischoff, D., Bister, B., Sussmuth, R. D., Pelzer, S., Wohlleben, W., Robinson, J. A. & Schlichting, I. (2002). *J. Biol. Chem.* **277**, 47476–47485.